U-Pb SHRIMP zircon dating of Grenvillian metamorphism in Western Sierras Pampeanas (Argentina): correlation with the Arequipa–Antofalla craton and constraints on the extent of the Precordillera Terrane

Cesar Casquet[1*], Robert J. Pankhurst[2], C. Mark Fanning[3], Edgardo Baldo[4], Carmen Galindo[1], Carlos W. Rapela[5], Jose M. González-Casado[6] and Juan A. Dahlquist[7]

[1] *Universidad Complutense Madrid, Dpto. Petrología y Geoquímica, 28040 Madrid, Spain*

[2] *British Geological Survey, Keyworth, Nottingham NG12 5GG, UK*

[3] *Research School of Earth Sciences, ANU, Camberra, ACT 200, Australia*

[4] *Universidad Nacional de Córdoba, Dpto. de Geología, 5000 Córdoba, Argentina*

[5] *CIG, Universidad Nacional de La Plata, Calle 1 No. 644, 1900 La Plata, Argentina*

[6] *Universidad Autónoma, Dpto. de Química Agrícola, Geología y Geoquímica, 28049 Madrid, Spain*

[7] *CRILAR-CONICET, 5301 Anillaco, La Rioja, Argentina*

Abstract

Metamorphism of Grenvillian age (*ca.* 1.2 Ga; U-Pb zircon dating) is recognized for the first time in the Western Sierras Pampeanas (Sierra de Maz). Conditions reached granulite facies (*ca.* 780ºC and *ca.* 780 MPa). Comparing geochronological and petrological characteristics with other outcrops of Mesoproterozoic basement, particularly in the northern and central Arequipa–Antofalla craton, we suggest that these regions were part of a single continental crustal block from Mesoproterozoic times, and thus autochthonous or parautochthonous to Gondwana.

Key words: Sierras Pampeanas, Argentina, metamorphism, U-Pb SHRIMP zircon dating, Grenville.

Introduction

The Sierras Pampeanas of Argentina, the largest outcrop of pre-Andean crystalline basement in southern South America, resulted from plate interactions along the proto-Andean margin of Gondwana, from as early as Mesoproterozoic to Late Paleozoic times (e.g., Ramos, 2004, and references therein). Two discrete Paleozoic orogenic belts have been recognized: the Early Cambrian Pampean belt in the eastern sierras, and the Ordovician Famatinian belt, which partially overprints it to the west (e.g., Rapela et al., 1998). In the Western Sierras Pampeanas, Mesoproterozoic igneous rocks (*ca.* 1.0–1.2 Ga) have been recognized in the Sierra de Pie de Palo (Fig. 1) (McDonough et al., 1993; Pankhurst and Rapela, 1998; Vujovich et al., 2004) that are time-coincident with the Grenvillian orogeny of eastern and northeastern North America (e.g., Rivers, 1997; Corriveau and van Breemen, 2000). These Grenvillian-age rocks have been considered to be the easternmost exposure of basement to the Precordillera Terrane, a supposed Laurentian continental block accreted to Gondwana during the Famatinian orogeny (Thomas and Astini, 2003, and references therein). However, the boundaries of this Grenvillian belt are still poorly defined, and its alleged allochthoneity has been challenged (Galindo et al., 2004). Moreover, most of the Grenvillian ages so far determined relate to igneous protoliths, and there is no conclusive evidence for a Grenvillian orogenic belt, other than inferred from petrographic evidence alone (Casquet et al., 2001). We provide here the first evidence, based on U-Pb SHRIMP zircon dating at Sierra de Maz, for a Grenville-age granulite facies metamorphism, leading to the conclusion that a continuous mobile belt existed throughout the proto-Andean margin of Gondwana in Grenvillian times.

Geological setting

The Sierra de Maz, along with the nearby sierras of Espinal, Ramaditas and Asperecitos (Fig. 1), defines a NNW–SSE trending belt of metamorphic rocks ranging from high-grade in the east to low-grade in the west. Three parallel domains can be discriminated in the field, separated by first-order shear zones (Fig. 1). The eastern domain consists of garnet-sillimanite migmatitic paragneisses, few marble outcrops and amphibolites. The central domain consists for the most part of medium grade (kyanite-sillimanite-garnet-staurolite) schists, quartzites, amphibolites and random marble outcrops. However, in the easternmost part of this domain in the Sierra de Maz there is a distinct sequence of hornblende - biotite – garnet gneisses, and biotite - garnet gneisses with some interleaved quartzites and scattered marble lenses. Relics of mafic grunulites and meta-peridotites are locally found within this sequence. Massif-type anorthosites are also found within this central domain, both in Maz and Espinal (Fig. 1) (Casquet et al., 2005) and are apparently hosted by the latter sequence of rocks. Other rock types of the central domain are orthogneisses and a still poorly known metaplutonic complex of meta-diorites to ortho-amphibolites apparently older than the anorthosites. The third domain, in the west, is formed by two low-grade metasedimentary sequences. One consists for the most part of garnet - chlorite schist with minor quartzites. The second is dominated by marbles, calc-silicate rocks and Ca-pelitic schist and is remarkably similar to the Neoproterozoic Difunta Correa sequence of the Sierra de Pie de Palo (Casquet et al., 2001; Rapela et al., 2005).

Porcher et al. (2004) reported Sm-Nd garnet–whole rock ages from eastern Sierra de Maz of 1039.9 ± 3.1 Ma and 969 ± 20 Ma, interpreted as recording a first thermal event. However, without leaching of garnet to remove apatite and other REE-bearing minerals, the meaning of these ages remains uncertain. This region underwent a pervasive tectono-thermal event during the Famatinian orogeny, between 435 and 450 Ma (Casquet et al., 2001, 2005, and unpublished data).

We focus here on the eastern part of the central domain, where high-grade rocks were probably host to the anorthosites and might thus preserve evidence of their pre-Famatinian history. An imbricated and folded sequence of schists, gneisses, quartzites, metabasites and serpentinite bodies crop out at Mina del Grafito (Fig.1): hydrothermal graphite was mined here in the past. We chose one schist (MAZ-6063) for U-Pb SHRIMP zircon dating and one metabasite (MAZ-6062) for assessing P-T conditions of metamorphism.

Samples description and conditions of metamorphism

MAZ-6063 is a garnet schist consisting of quartz, biotite, garnet and plagioclase with accessory rutile, ilmenite, zircon, monazite and apatite. Biotite is abundant and defines a foliation that wraps around garnets. Garnet porphyroblasts are subhedral to anhedral and are partially replaced by matrix biotite; they have large cores rich in inclusions of matrix minerals, particularly rutile, and inclusion-free mantles. The garnet is chemically quite homogeneous ($alm_{55.7–64.3}$, $prp_{26.0–34.4}$, $grs_{6.4–8.0}$, $sps_{1.4–2.0}$); plagioclase is unzoned ($an_{33.4–34.5}$, $ab_{64.5–66.3}$, $or_{0.2–1.0}$) and variably sericitized.

MAZ-6062 is a fine-grained amphibolitized basic granulite with a predominantly granoblastic texture. It consists of plagioclase ($an_{47.0–82.4}$, $ab_{17.0–52.8}$, $or_{0.5–1.0}$), garnet ($alm_{48.2–53.9}$, $prp_{24.1–28.4}$, $grs_{19.1–22.2}$, $sps_{1.9–2.5}$), clinopyroxene, orthopyroxene, Mg-hornblende, biotite and accessory apatite and ilmenite. Its petrography suggests two metamorphic events: an older granulite facies one (M1) forming Opx + Cpx + $Pl_1(an_{70\text{-}82})$ + Grt_1 + Bt, and a younger garnet amphibolite facies one (M2) that produced Hbl + Pl_2 + Grt_2 , the latter as idiomorphic overgrowths on Grt_1 (Fig. 2;

mineral abreviations after Kretz, 1983). Pressure and temperature for M1 were assessed from the presumed equilibrium mineral compositions using Thermocalc v. 3.1 (Powell & Holland, 1988), and yielded P = 780 ± 140 MPa, and T = 775 ± 95ºC (Table 1). The pressure suggest a crustal depth of *ca.* 29 km for this event.

U-Pb SHRIMP geochronology

A zircon concentrate was obtained from MAZ-6063. The zircons are round to sub-round in shape, mostly *ca.* 100 μm in diameter. Cathodoluminescence (CL) images reveal cores (simply or complexly zoned, often quite small) mantled by complete overgrowths that often represent >50 % of the grain volume (Fig. 3). The latter are of two types: thick patchily sector-zoned (‘soccer-ball’) zircon, thought to signify high-grade metamorphism at a deep crustal level (e.g., Vavra et al., 1999), and clearer, unzoned metamorphic overgrowths. They are rarely identifiable on the same grain, but in such cases the ‘soccer-ball’ zoning is innermost; there often appears to be a gradation between the two types. On many grains there is also a thin outermost rim of lower luminescence (<< 10 microns in width).

U-Pb zircon dating was carried out by sensitive high resolution ion microprobe (SHRIMP) using SHRIMP II at ANU, Canberra, targeting 20 areas, including 7 cores and 13 overgrowths (Table 2 and fig. 3). The cores have $^{207}Pb/^{206}Pb$ ages ranging from *ca*. 1000 to 2000 Ma, with apparent peaks at ~1700 and ~1880 Ma. Two cores with younger ages of 1178 ± 27 and 1063 ± 57 Ma could represent major radiogenic Pb-loss during metamorphism. Nine of the ten mantle overgrowths analysed have $^{207}Pb/^{206}Pb$ ages ranging between 1130 and 1370 Ma (ignoring one imprecise result of 1000 Ma), with a weighted mean of 1208 ± 28 Ma (MSWD = 3.4). The “soccer ball”-zoned domains gave ages of 1180–1230 Ma, within this range, and the weighted mean includes both types (but see below). The thin outermost rims were too thin to analyses and, in view of the interpretation below, it is thought that they might represent Ordovician metamorphism.

Interpretation of zircon ages

The simplest interpretation of the U-Pb data is that the original sediment had a late Palaeoproterozoic provenance and underwent high-grade metamorphism in the lower crust at about 1200 Ma. Slight radiogenic Pb-loss could have occurred as the rock underwent partial exhumation at 1000–1100 Ma. The depositional age is poorly constrained since the number of grains dated is less than that usually considered necessary for a full provenance analysis, but must be between the age of metamorphism and that of the youngest detrital cores at 1.7 Ga.

With respect to the metamorphic mantled overgrowths analysed, statistical mixture modelling of the data (using ISOPLOT) suggests one component at *ca.* 1230 Ma and another at *ca.* 1180 Ma (with possibly a third slightly younger yet, though this is probably a consequence of radiogenic Pb loss). Nevertheless, the overlap in the ages between the two types of metamorphic overgrowths suggests that any two such events occurred within a relatively short time interval (i.e., within 50 Ma). On the basis of the evenness and completeness of the mantled overgrowths on most grains, the grain-shape is interpreted to be the result of metamorphism rather than surface transport. Therefore the rock may have been partially exhumed during deep crustal metamorphism, withouth a major drop in temperature, to account for gradation between the two types of overgrowths. A deep crustal granulite facies metamorphism (M1) has been recognized from MAZ-6062, and so it is highly probable that the ‘soccer-ball’ zircon overgrowths formed “in situ” and the age of 1208 ± 28 Ma constrains the timing of that M1 event. The second metamorphism seen in MAZ-6062 (M2) is not unambiguously dated: it seems most likely that it was the result of partial exhumation immediately following deep crustal metamorphism, without a major drop in temperature, which would account for gradation between the two types of mantling overgrowths. Alternatively, M2 could relate to the undated thin outer zircon rims (Famatinian?).

Discussion

The age of 1208 ± 28 Ma of the M1 metamorphic event is broadly coincident with the age of the Elzevirian accretionary orogenic event recorded in the Grenvillian Province of eastern Canada (~ 1250 – 1190 Ma; Rivers, 1997). Corrieveau and van Breemen (2000) provided evidence from metamorphic P-T conditions and geochronology that the Grenvillian continent-continent collisional orogeny was initiated at the end of the Elzevirian at *ca.* 1.2 Ga. In consequence we consider that the M1 metamorphic recognized for the first time in the Sierra de Maz can be taken as an early Grenvillian event. The Grenvillian orogeny ended at between 1.0 Ga and 0.85 Ga (Rivers, 1997).

Evidence of a Grenvillian tectonothermal event in the western sierras Pampeanas is also found in the Sierra de Pie de Palo, and in the Arequipa–Antofalla craton (Fig. 1). In the first, metamorphism older than *ca.* 1.1 Ga was inferred from combined U-Pb SHRIMP detrital zircon data and petrographic evidence (Casquet et al., 2001). The Sierra de Pie de Palo exhibits stacking of Famatinian nappes formed by Mesoproterozoic meta-igneous rocks with ages of *ca.* 1.0–1.1 Ga (McDonough et al., 1993; Pankhurst and Rapela, 1998) and metasedimentary rocks, beneath a Neoproterozoic metasedimentary cover (Casquet et al., 2001; Galindo et al., 2004). The lowermost unit is interpreted to represent a Mesoproterozoic oceanic arc/back arc complex of *ca.* 1.2 Ga (Vujovich et al., 2004, and references therein). Thus tectonothermal activity took place here in Grenvillian times (*ca.* 1.0–1.2 Ga). Pre-Famatinian metamorphism reaching high-grade migmatitic conditions (686 ± 40 MPa, 790 ± 17ºC) has only been recognized in the basement of the upper nappes (Casquet et al., 2001). These P-T values are within error of those inferred for M1 in eastern Sierra de Maz, thus strengthening the idea that both regions underwent the same metamorphic event. Within the Western Sierras Pampeanas, orthogneisses of Grenvillian age have also been found in the Sierra de Umango (Varela et al,. 2004), northwest of the Sierra de Espinal (Fig. 1).

The Arequipa–Antofalla craton (Ramos, 1988) lies to the northwest of the Sierras Pampeanas in Peru, Bolivia, and northern Chile and Argentina (Fig. 1), and exhibits scattered inliers of rocks of Proterozoic and Early Paleozoic age, exposed through the Andean Mesozoic to Cenozoic sedimentary and volcanic cover sequence. It was apparently accreted to the Amazonian craton to the east during the Sunsas orogeny at *ca.* 1.0–1.2 Ga according to Loewy et al. (2004). The northern and central parts consist of Mesoproterozoic metasedimentary rocks, metavolcanic rocks and orthogneisses, the latter with peak U-Pb zircon crystallization ages of *ca.* 1.8–1.9 Ga in the north and *ca.* 1.05–1.25 Ga in the central region (Damm et al., 1990; Wasteneys et al., 1995; Tosdal, 1996; Loewy et al., 2004). Grenville-age medium- to high-grade (granulite) metamorphism and deformation overprinted both domains between *ca.* 1200 and 950 Ma (Wasteneys at al., 1995; Loewy et al., 2004), and the region underwent Famatinian metamorphism and magmatism between 470 and 440 Ma (Loewy et al., 2004).

From the above, the similarities between central and northern Arequipa–Antofalla craton and the Western Sierras Pampeanas are evident, the igneous event at 1.8 Ga to 1.9 Ga being recorded by the zircon cores of MAZ-6063 with $^{207}Pb/^{206}Pb$ peak ages at ~1700 and ~1880 Ma. This suggests that the source of MAZ-6063 zircons was – at least in part – an igneous province similar to the northern and central Arequipa–Antofalla orthogneisses. Still more important is the conclusion that magmatism and regional metamorphism attaining granulite facies conditions occurred in both regions between *ca.* 1.2 Ga and *ca.* 1.0 Ga, suggesting that they were probably part of the same mobile belt of Grenvillian age. These parallels extend to the existence of Grenvillian massif-type anorthosites in both the Western Sierras Pampeanas (Casquet et al., 2005) and the northern Arequipa–Antofalla domain (Martignole et al., 2005), and both regions were reworked by Famatinian metamorphism at *ca.* 450 Ma. Thus it is suggested that these two regions were part of a single continental crustal block from Mesoproterozoic times onwards (Fig. 1). The Sierra de Pie de Palo pre-Famatinian basement was probably part of this same Grenville-age mobile belt, although it contains an ophiolitic assemblage that has not been recognized so far in the northwestern Sierras Pampeanas or – as far as we are aware – in the Arequipa–Antofalla craton. Thus, like the Arequipa–Antofalla block (e.g., Loewy et al., 2004) the Western Sierras Pampeanas must be considered autochthonous or parautochthonous to the pre-Famatinian margin of Gondwana, and not part of the Precordillera terrane, in further agreement with recent isotope and zircon provenance evidence (Galindo et al., 2004; Vujovich et al., 2004).

Acknowledgements

This work was supported by Spanish (BTE2001-1486) and Argentine public grants. R.J.P. acknowledges a NERC Small Research Grant.

References

Casquet, C., Baldo, E., Pankhurst, R.J., Rapela, C.W., Galindo, C., Fanning, C.M. and Saavedra, J. (2001) Involvement of the Argentine Precordillera Terrane in the Famatinian mobile belt: Geochronological (U-Pb SHRIMP) and metamorphic evidence from the Sierra de Pie de Palo. Geology, v. 29, pp. 703-706.

Casquet, C., Rapela, C.W., Pankhurst, R.J., Galindo, C., Dahlquist , J., Baldo, E.G., Saavedra, J., González Casado, J.M., Fanning, C.M. (2005) Grenvillian massif-type anorthosites in the Sierras Pampeanas. J. Geol. Soc. London, v. 162, pp. 9-12.

Corrievau, L. and van Breemen, O. (2000) Docking of the Central Metasedimentary Belt to Laurentia in geon 12: evidence from the 1.17 – 1.16 Ga Chevreuil intrusive suite and host gneisses, Quebec. Can. J. Earth. Sci., 37, pp. 253-269.

Damm, K.W., Pichowiak, S., Harmon, R.S., Todt, W., Kelley, S., Omarini, R. and Niemeyer, H. (1990) Pre-Mesozoic evolution of the central Andes; the basement revisited. Geol. Soc. Amer. Spec. Paper, v. 241, pp. 101-126.

Galindo, C., Casquet, C., Rapela, C., Pankhurst, R.J., Baldo, E. and Saavedra, J. (2004) Sr, C and O isotope geochemistry and stratigraphy of Precambrian and Lower Paleozoic carbonate sequences from the Western Sierras Pampeanas of Argentina: tectonic implications. Precambrian Res., v.131, pp. 55-71.

Kretz, R. (1983) Symbols for rock-forming minerals. American Mineralogist, v. 68, pp. 277-279.

Loewy, S.L., Connelly, J.N. and Dalziel, I.W.D. (2004) An orphaned basement block: the Arequipa–Antofalla Basement of the central Andean margin of South America. Geol. Soc. Amer. Bull., v. 116, pp. 171-187.

Martignole, J., Stevenson, R. and Martelat, J.E. (2005) A Grenvillian anorthosite-mangerite-charnockite-granite suite in the basement of the Andes: the Ilo AMCG site (southern Peru). ISAG, Barcelona, Extended abstracts, pp. 481-484.

McDonough, M.R., Ramos, V.A., Isachsen, C.E., Bowring, S.A. and Vujovich, G.I. (1993) Edades preliminares de circones del basamento de la Sierra de Pie de Palo, Sierras Pampeanas occidentales de San Juán: sus implicancias para el supercontinente proterozoico de Rodinia, 12º Cong. Geol. Argentino, Actas, 3, pp. 340-342.

Pankhurst, R.J. and Rapela, C.W. (1998) Introduction, In Pankhurst, R.J. and Rapela, C.W. (Eds.), The Proto-Andean Margin of Gondwana. Geol. Soc. Spec. Pub., v. 142, pp. 1-9.

Porcher, C.C., Fernandes, L.A.D., Vujovich, G.I. and Chernicoff, C.J. (2004) Thermobarometry, Sm/Nd ages and geophysical evidence for the location of the suture zone between Cuyania and Pampia terranes. In Vujovich, G.I., Fernandes, L.A.D. and Ramos, V.A. (Eds.) Cuyania: an exotic block to Gondwana. Gondwana Res., v. 7, pp. 1057-1076.

Powell, R. and Holland, T.J.B. (1988) An internally consistent dataset with uncertainties and correlations: 3. Applications to geobarometry, worked examples and a computer program. J. Metam. Geol., v. 6, pp. 173-204.

Ramos, V.A (1988) Tectonics of the Late-Proterozoic – Early Paleozoic: a collisional history of Southern South America. Episodes, v. 11, pp. 168-174.

Ramos V.A. (2004) Cuyania, an exotic block to Gondwana: Review of a historical success and the present problems. In Vujovich, G.I., Fernandes, L.A.D. and Ramos, V.A. (Eds.) Cuyania: An exotic block to Gondwana. Gondwana Res., v. 7, pp. 1009-1026.

Ramos, V.A. and Vujovich, G.I. (1993) Alternativas de la evolución del borde occidental de America del Sur durante el Proterozoico. Rev. Brasil. Geoc., v. 23, pp. 194-200.

Rapela, C.W., Pankhurst, R.J., Casquet, C., Fanning, C.M., Galindo, C., Baldo, E. (2005) Datación U-Pb SHRIMP de circones detríticos en para-anfibolitas neoproterozoicas de la secuencia Difunta Correa (Sierras Pampeanas Occidentales, Argentina). Geogaceta, 38, pp. 227-230.

Rivers, T. (1997) Lithotectonic elements of the Grenville Province: review and tectonic implications. Precambrian Res., 86, 3-4, pp. 117-154.

Rapela, C.W., Pankhurst, R.J., Casquet, C., Baldo, E., Saavedra, J. and Galindo, C. (1998) Early evolution of the proto-Andean margin of South America. Geology, v. 26, pp. 707-710.

Thomas, W.A. and Astini, R.A. (2003) Ordovician accretion of the Argentine Precordillera terrane to Gondwana: a review. J. S. Amer. Earth Sci., v. 16, pp. 67-79.

Tosdal, R.M. (1996) The Amazon-Laurentian connection as viewed from the Middle Proterozoic rocks in the central Andes, western Bolivia and northern Chile. Tectonics, v. 15, pp. 827-842.

Varela, R., Sato, A., Basei, M.A.S. and Siga Jr., O. (2004) Proterozoico medio y Paleozoico inferior de la Sierra de Umango, antepais andino (29ºS), Argentina: edades U-Pb y caracterizaciones isotópicas. Rev. Geol. Chile, v. 30, pp. 265-284.

Vavra, G., Schmid, R. and Gebaüer, D. (1999) Internal morphology, habit and U-Th-Pb microanalysis of amphibolite-to-granulite facies zircon: geochronology of the Ivrea Zone (Southern Alps). Contr. Mineral. Petrol., v. 134, pp. 380-404.

Vujovich, G.I., Van Staal, C.R. and Davis, W. (2004) Age constraints and the tectonic evolution and provenance of the Pie de Palo Complex, Cuyania composite terrane, and the Famatinian orogeny in the Sierra de Pie de Palo, San Juán, Argentina. Gondwana Res., v. 7, pp. 1041-1056.

Wasteneys, H.A., Clark, A.H., Farrar, E. and Langridge, R.J. (1995) Grenvillian granulite-facies metamorphism in the Arequipa massif: a Laurentia- Gondwana link. Earth Planet. Sci. Lett., v. 132, pp. 63-73.

Figure and table captions

Fig. 1. Location of the Sierras Pampeanas and of the Arequipa–Antofalla craton (AAC) (based on Ramos & Vujovich, 1993). WSP, Western Sierras Pampeanas; ESP, Eastern Sierras Pampeanas; PC, Argentine Precordillera; *SPP*, Sierra de Pie de Palo. Main figure shows a geological sketch map of the Sierra de Maz and surrounding areas referred to in the text. Crystalline basement: 1, Eastern domain; 2, Central domain; 3, Western Domain; 4, anorthosite massifs; 5, Famatinian plutons; 6, Upper Paleozoic sedimentary cover; Areas withouth ornaments: Mesozoic and Quaternary sedimentary cover; A, ductile shear zones; B, thrusts; C; main foliation trend lines. Mina del Grafito is the sampling location.

Fig. 2. Photomicrographs of retrogressed mafic granulite sample MAZ-6062. (A) Retrograde hornblende (M2) is interstitial to biotite + orthopyroxene + garnet (M1). Euhedral garnet overgrowths probably formed coeval with hornblende during the M2 metamorphic event. Garnet encloses oriented tiny crystals of biotite but never hornblende. (B) Euhedral garnet crystals with inclusions of biotite and ore minerals are set in a large biotite crystal. Hornblende here is interstitial to clinopyroxene and biotite. Abreviations after Kretz (1983).

Fig. 3. U–Pb SHRIMP zircon geochronology of sample MAZ-6063. The upper part is a representative cathodoluminescence image of the sectioned zircon grains, showing some of the SHRIMP analysis spots with calculated ages. The lower part is a Wetherill Concordia plot of the data: the cores have the 1700-1900 Ma provenance ages, whereas the metamorphic mantles grew during the Grenville-age event at ca. 1200 Ma. See text and Table 2 for further details.

Table 1. Mineral compositions (MAZ-6062) chosen to retrieve P-T conditions for M1 metamorphism using Thermocalc v. 3.1 (Powell and Holland, 1988).

Table 2. Summary of SHRIMP U-Pb zircon results for sample MAZ-6063.

.

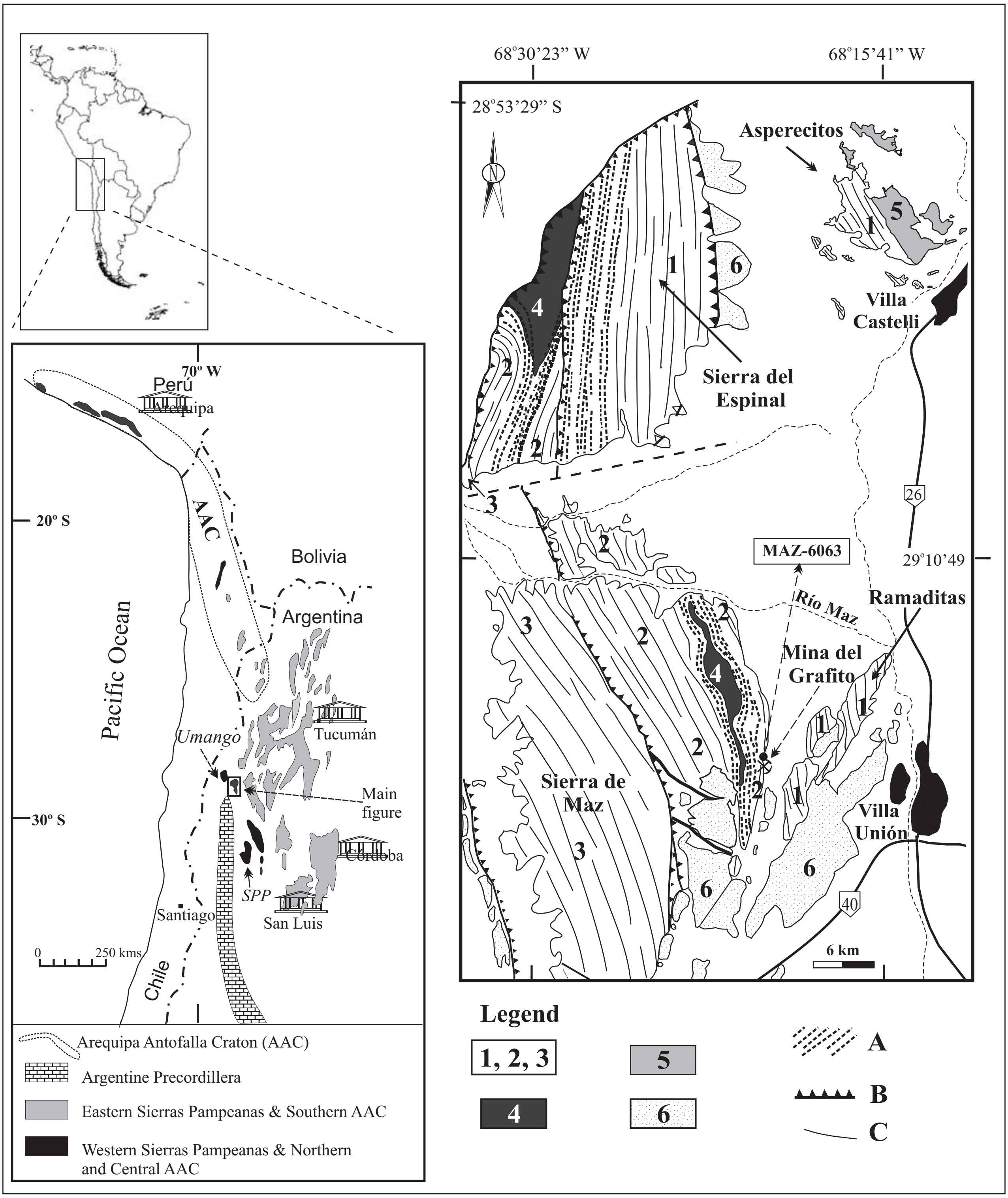

Peru
Arequipa
70º W
20º S
30º S
AAC
Bolivia
Argentina
Pacific Ocean
Tucumán
Umango
Main figure
Córdoba
SPP
San Luis
Santiago
Chile
0 250 kms
Arequipa Antofalla Craton (AAC)
Argentine Precordillera
Eastern Sierras Pampeanas & Southern AAC
Western Sierras Pampeanas & Northern and Central AAC
68º30'23" W
68º15'41" W
28º53'29" S
29º10'49
Asperecitos
Villa Castelli
Sierra del Espinal
MAZ-6063
Río Maz
Ramaditas
Mina del Grafito
Sierra de Maz
Villa Unión
26
40
6 km
Legend
1, 2, 3
4
5
6
A
B
C

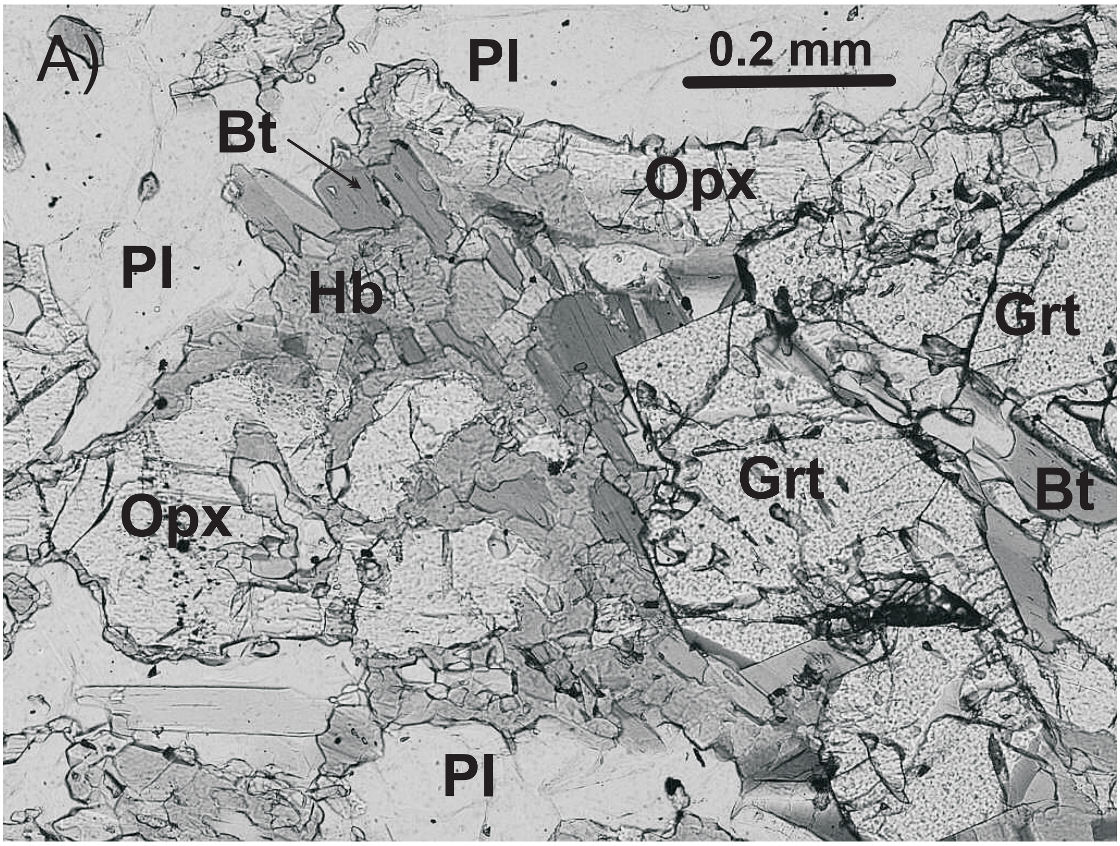
A)
Pl
0.2 mm
Bt
Opx
Pl
Hb
Grt
Grt
Bt
Opx
Pl

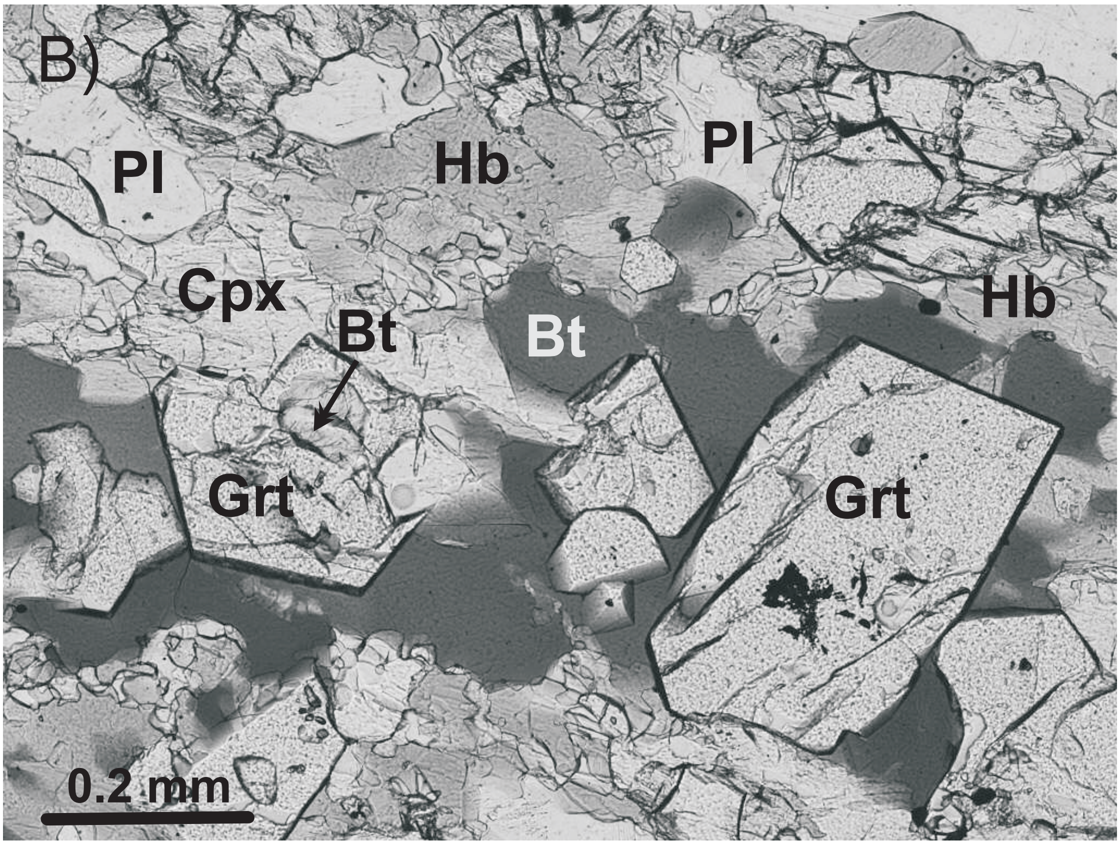
B)
Pl
Hb
Pl
Cpx
Bt
Bt
Hb
Grt
Grt
0.2 mm

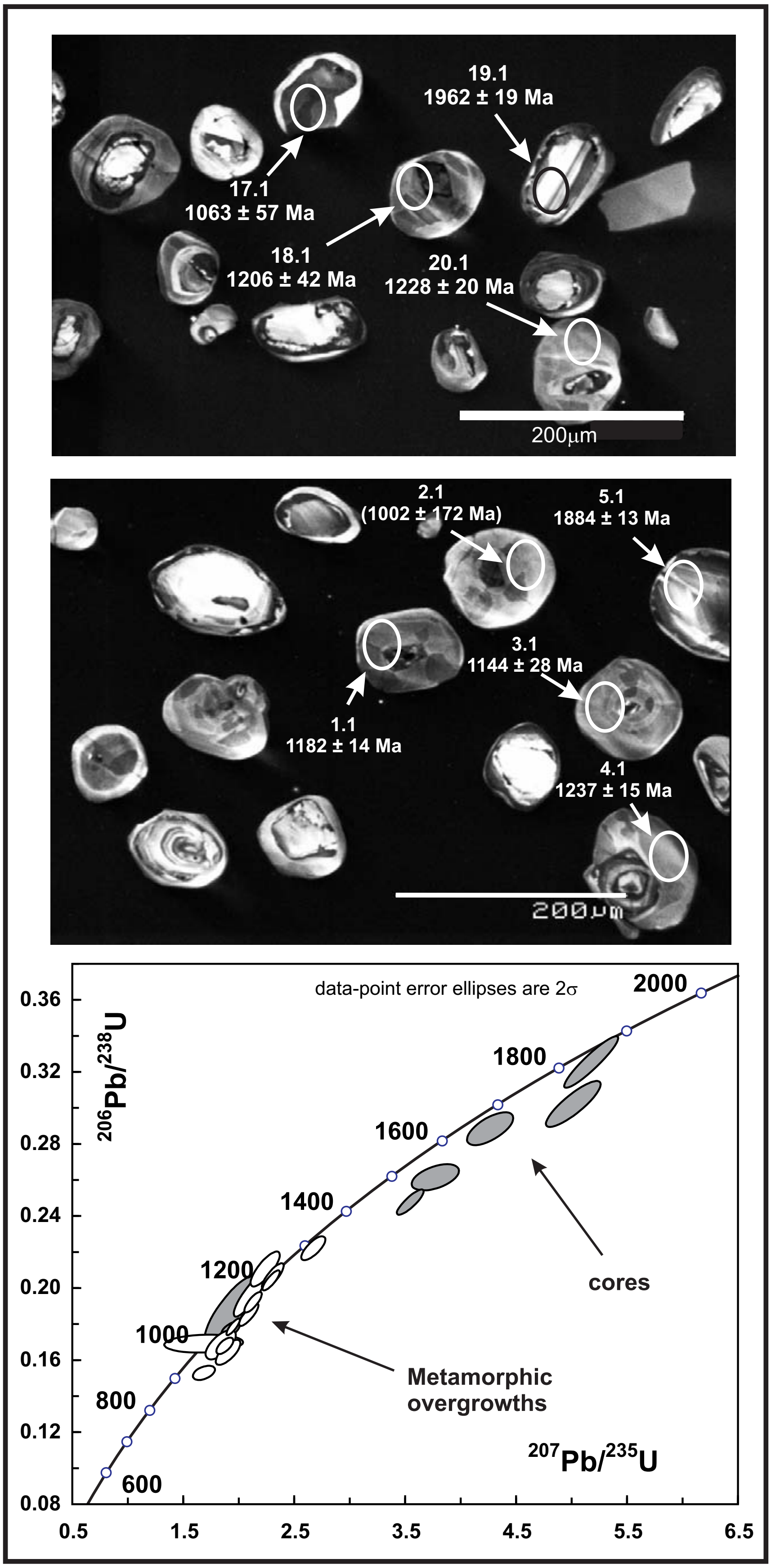
17.1
1063 ± 57 Ma
18.1
1206 ± 42 Ma
19.1
1962 ± 19 Ma
20.1
1228 ± 20 Ma
200μm
2.1
(1002 ± 172 Ma)
5.1
1884 ± 13 Ma
3.1
1144 ± 28 Ma
1.1
1182 ± 14 Ma
4.1
1237 ± 15 Ma
200μm
data-point error ellipses are 2σ
2000
1800
1600
1400
1200
1000
800
600
cores
Metamorphic
overgrowths
206Pb/238U
207Pb/235U
0.36
0.32
0.28
0.24
0.20
0.16
0.12
0.08
0.5
1.5
2.5
3.5
4.5
5.5
6.5

Table 1: Mineral compositions (MAZ-6062) chosen to retrieve P-T conditions for M1 metamorphism using Thermocalc v 3.1 (Powell and Holland, 1988)

Mineral	**Grt**		**Cpx**	**Opx**		**Pl**		**Bt**
Anal. Nº	6062-72		6062-57	6062-77		6062-62		6062-78
SiO_2	39.98		51.67	53.80		52.12		36.42
TiO_2	0.01		0.10	0.00		0.02		4.90
Al_2O_3	21.85		1.41	1.02		31.14		14.90
Cr_2O_3	0.00		0.10	0.07		0.00		0.26
FeO	22.38		6.74	21.05		0.13		12.43
MnO	0.91		0.10	0.32		0.00		0.00
NiO	0.03		0.02	0.05		0.00		0.00
ZnO	0.03		0.10	0.11		0.00		0.00
MgO	7.30		14.38	21.83		0.00		14.88
CaO	7.78		23.61	0.52		14.55		0.01
Na_2O	0.02		0.22	0.01		1.65		0.03
K_2O	0.00		0.00	0.00		0.10		10.05
F	0.00		0.00	0.00		0.00		0.03
Cl	0.00		0.00	0.00		0.00		0.00
Total	100.29		98.45	98.78		99.70		93.97
Cat.	12 O	Cat.	6 O	6 O	Cat.	32 O	Cat	24 O
TSi	3.06	TSi	1.94	2.03	Si	9.44	Si	5.739
TAl	0.00	TAl	0.06	0.00	Al	6.64	Al^{IV}	2.26
Al^{VI}	1.97	M1Al	0.01	0.05	Ti	0.00	Al^{VI}	0.51
Ti	0.00	M1Ti	0.00	0.00	Fe^2	0.02	Ti	0.58
Cr	0.00	$M1Fe^2$	0.18	0.00	Mn	0.00	Fe^2	1.64
Fe^2	1.43	M1Cr	0.00	0.00	Mg	0.00	Cr	0.03
Mg	0.83	M1Mg	0.81	0.95	Ca	2.82	Mn	0.00
Mn	0.06	M1Ni	0.00	0.00	Na	0.58	Mg	3.50
Ca	0.64	M2Mg	0.00	0.28	K	0.02	Ca	0.00
Na	0.00	$M2Fe^2$	0.03	0.66	**An**	**82.40**	Na	0.01
Grt end members		M2Mn	0.00	0.01			K	2.02
Alm	**48.31**	M2Ca	0.95	0.02			**XMg**	**68.00**
Gross	**21.52**	M2Na	0.02	0.00				
Pyrope	**28.10**	M2K	0.00	0.00				
Spess	**1.99**	**XMg**	**79.09**	**63.84**				

Table *2* . Summary of SHRIMP U-Pb zircon results for sample MAZ 6063.

Grain. spot	U (ppm)	Th (ppm)	Th/U	Pb* (ppm)	$^{204}Pb/^{206}Pb$	f_{206} %	Radiogenic Ratios $^{206}Pb/^{238}U$	±	$^{207}Pb/^{235}U$	±	$^{207}Pb/^{206}Pb$	±	ρ	Age (Ma) $^{206}Pb/^{238}U$	±	$^{207}Pb/^{206}Pb$	±	% Disc	
1.1	788	30	0.04	121	0.000125	0.21	0.1785	0.0019	1.954	0.025	0.0794	0.0006	0.834	1059	10	1182	14	12	rim
2.1	278	14	0.05	40	0.000084	0.14	0.1692	0.0020	1.693	0.145	0.0726	0.0062	0.139	1007	11	1002	172	-1	rim
3.1	441	17	0.04	74	0.000049	0.08	0.1965	0.0050	2.111	0.062	0.0779	0.0011	0.873	1157	27	1144	28	-1	rim
4.1	293	13	0.05	51	0.000044	0.07	0.2042	0.0023	2.298	0.031	0.0816	0.0006	0.824	1198	12	1237	15	3	rim
5.1	162	234	1.45	45	0.000031	0.05	0.3255	0.0058	5.172	0.100	0.1153	0.0008	0.929	1816	28	1884	13	4	core
6.1	224	22	0.10	37	0.000061	0.10	0.1922	0.0023	2.134	0.032	0.0805	0.0008	0.788	1133	12	1209	18	7	rim
7.1	613	15	0.02	93	0.000035	0.06	0.1767	0.0019	1.930	0.034	0.0792	0.0011	0.613	1049	10	1178	27	12	core
8.1	618	48	0.08	90	0.000244	0.41	0.1679	0.0018	1.880	0.031	0.0812	0.0010	0.654	1001	10	1227	25	23	rim
9.1	248	323	1.30	53	0.000065	0.10	0.2477	0.0029	3.545	0.049	0.1038	0.0008	0.847	1426	15	1693	14	19	core
10.1	153	44	0.29	29	0.000104	0.17	0.2221	0.0027	2.673	0.044	0.0873	0.0010	0.741	1293	14	1367	22	6	rim
11.1	387	24	0.06	87	0.000021	0.03	0.2615	0.0030	3.771	0.087	0.1046	0.0021	0.493	1498	15	1707	37	14	core
12.1	239	174	0.73	59	0.000070	0.11	0.2884	0.0038	4.263	0.085	0.1072	0.0016	0.655	1634	19	1752	28	7	core
13.1	518	31	0.06	73	0.000054	0.09	0.1643	0.0028	1.912	0.046	0.0844	0.0014	0.722	981	16	1302	32	33	rim
14.1	462	22	0.05	84	0.000038	0.06	0.2105	0.0040	2.243	0.053	0.0773	0.0011	0.802	1232	21	1128	28	-8	rim
15.1	677	37	0.05	98	-	<0.01	0.1684	0.0033	1.843	0.055	0.0794	0.0018	0.657	1003	18	1182	45	18	rim
16.1	681	31	0.05	109	0.000154	0.26	0.1852	0.0026	2.099	0.035	0.0822	0.0008	0.822	1095	14	1250	19	14	rim
17.1	904	17	0.02	146	-	<0.01	0.1880	0.0077	1.939	0.097	0.0748	0.0021	0.820	1111	42	1063	57	-4	core
18.1	742	67	0.09	99	0.000730	1.22	0.1529	0.0016	1.693	0.040	0.0803	0.0017	0.452	917	9	1206	42	31	rim
19.1	159	66	0.41	41	0.000004	0.01	0.3021	0.0052	5.014	0.101	0.1204	0.0013	0.855	1702	26	1962	19	15	core
20.1	281	16	0.06	50	0.000049	0.08	0.2066	0.0030	2.314	0.041	0.0813	0.0008	0.815	1211	16	1228	20	1	rim

Notes :
1. Uncertainties given at the one σ level.
2. f_{206} % denotes the percentage of ^{206}Pb that is common Pb.
3. Correction for common Pb made using the measured $^{204}Pb/^{206}Pb$ ratio.
4. For % Disc., 0% denotes a perfectly concordant analysis.